

The IgG Binding Site of Human FcγRIIIB Receptor Involves CC' and FG Loops of the Membrane-proximal Domain*

(Received for publication, September 25, 1995)

Anu Tamm, Alexander Kister‡§, K. Ulrich Nolte, J. Engelbert Gessner, and Reinhold E. Schmidt†¶

From the Department of Clinical Immunology, Hannover Medical School, Konstanty-Gutschow Straße 8, 30625 Hannover, Federal Republic of Germany and the ‡Laboratory of Immunobiology, Dana Farber Cancer Institute, Boston, Massachusetts 02115

Fcγ receptors for the Fc part of IgG are the mediators for antibody effector functions. FcγRIII and FcγRII are low affinity receptors that, through the interaction with immune complexes, initiate a variety of immunological responses, such as phagocytosis, antibody-dependent cellular cytotoxicity, and release of inflammatory mediators. We set out to define the IgG binding site on human FcγRIII. We assumed that potential β-turns in Ig-like domains are the most probable determinants for ligand binding, and chimeric FcγRIIIB/FcεRI receptors as well as single residue mutants were constructed in these regions of FcγRIIIB. Substitution of four amino acids in the membrane-proximal domain (Gln¹²⁶, Arg¹⁵⁶, Lys¹⁶², Val¹⁶⁴) resulted in decreased binding of human IgG1. Lys¹⁶² and Val¹⁶⁴ were found also to be crucial for the interaction with the IgG-binding inhibitory monoclonal antibody 3G8. In a putative three-dimensional model constructed in this study, these residues map on the CC' loop (Gln¹²⁶), on F β-sheet (Arg¹⁵⁶), and on the FG loop (Lys¹⁶², Val¹⁶⁴). Our data are consistent with the study about human FcγRII (Hulett, M. D., Witort, E., Brinkworth, R. I., McKenzie, I. F. C., and Hogarth, P. M. (1994) *J. Biol. Chem.* 269, 15287–15293), suggesting that common structural determinants, i.e. FG loop or the GFC surface of the membrane-proximal domain, can be involved in interactions with IgG by both low affinity receptor classes FcγRII and FcγRIII.

Fcγ receptors constitute a group of membrane proteins that interact with IgG Fc regions. The three classes of human Fcγ receptors (FcγRI, FcγRII, FcγRIII) belong to the Ig gene superfamily and are widely expressed in hematopoietic cell lineages (2–5). FcγRI (CD64) binds IgG with high affinity, whereas FcγRII (CD32) and FcγRIII (CD16) are low affinity receptors, interacting predominantly with immune complexes of the IgG3 and IgG1 subclasses (6, 7).

Human class III receptors are represented by two isoforms that differ in their membrane anchors (8), expression patterns, and affinities to IgG. The transmembrane FcγRIIIA (9) receptor is expressed on NK cells, macrophages, on subsets of monocytes, and T cells in association with dimers of the γ-chain of FcεRI (10–12) and/or the ζ-chain of T cell receptor (13). Expression of the glycosylphosphatidylinositol-anchored FcγRIIIB iso-

form is restricted to neutrophils (8, 14–16). Tissue-specific expression of the two isoforms can be regulated at the transcriptional level (17, 18). FcγRIIIA binds IgG1 and IgG3 complexes with higher affinity ($K_a \approx 3 \times 10^7 \text{ M}^{-1}$) than the B isoform ($K_a \leq 10^7 \text{ M}^{-1}$) and is able to interact with monomeric IgG (19–21). FcγRIIIB is represented by two allelic forms, NA1 and NA2, which can be detected with certain specific CD16 monoclonal antibodies (22, 23). NA1 and NA2 (24) differ in their glycosylation patterns (25) and in their ability to trigger phagocytosis by neutrophils (26, 27).

The Ig-binding extracellular regions of Fc receptors contain two (FcγRII, FcγRIII, FcεRI) or three (FcγRI) Ig-like disulfide-bonded domains (2–5) composed of seven antiparallel β-sheets (28). Loops between the β-sheets are likely to be involved in interactions with the ligands.

The membrane-proximal domain is crucial for IgG binding by most of the Fc receptors studied, i.e. human FcγRII (1, 29, 30), human FcεRI (30–32), mouse FcγRII (33, 34), and rat FcεRI (31). The membrane-distal domain of FcγRIIIB, when fused to domains 3–5 of ICAM-1, did not react with IgG (35). Thus, to identify the IgG binding sites of FcγRIII, we focused on the second, membrane-proximal domain of FcγRIIIB. We predicted potential β-turn regions of the second Ig-like domain with the aid of the PC Gene program, and within these regions, amino acid residues were exchanged with the equivalent ones in the α-chain of the human high affinity receptor for IgE, FcεRI (36). The resulting chimeric FcγRIII/FcεRI receptors should show diminished IgG binding affinity, since the extracellular part of FcεRI reveals significant amino acid identity (41%) with FcγRIIIB, but FcεRI does not interact with IgG (30).

Chimeric FcγRIII/FcεRI receptors revealed several regions on FcγRIIIB (amino acids 125–127, 152–158, 160–163), substitution of which resulted in decreased interaction with IgG. Following single residue mutagenesis and molecular modeling of the receptor indicated that amino acids critical for ligand binding are apparently located on the loops connecting C and C' β-sheets (Gln¹²⁶) as well as F and G β-sheets (Lys¹⁶², Val¹⁶⁴) and on the F β-sheet (Arg¹⁵⁶) all on the second extracellular domain of FcγRIIIB. These residues may constitute one discontinuous binding area on the GFC β-sheet surface for the ligand, IgG1 or IgG3 complexes. This was further supported by the finding that the epitope for the IgG-binding inhibitory monoclonal antibody (mAb)¹ 3G8 (37) was localized on the same FG loop of the membrane-proximal domain.

MATERIALS AND METHODS

cDNAs and mAbs—The wild-type cDNA for the FcγRIIIB gene, cloned into the pCDM8 expression vector (14), was provided by Dr. B. Seed (Harvard Medical School, Boston, MA).

* This work was supported by Deutsche Forschungsgemeinschaft Grant SFB 244/A09. The costs of publication of this article were defrayed in part by the payment of page charges. This article must therefore be hereby marked "advertisement" in accordance with 18 U.S.C. Section 1734 solely to indicate this fact.

§ Current address: Dept. of Mathematics, Hill Center, Rutgers University, New Brunswick, NJ 08903.

¶ To whom correspondence should be addressed. Tel.: 49-511-532-6656; Fax: 49-511-532-9067.

¹ The abbreviations used are: mAb, monoclonal antibody; wt, wild type; bp, base pair.

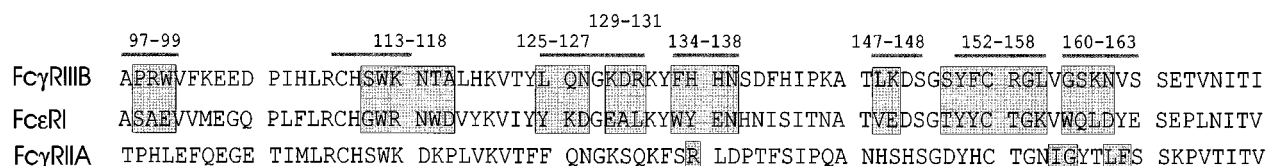


Fig. 1. Alignment of the membrane-proximal domains of hFcγRIIIB, hFcεRIα, and hFcγRIIA. Locations of the regions of highest β-turn probability in FcγRIIIB predicted by the Chou and Fasman method are indicated as gray bars over the sequence. Chimeric FcγRIIIB/FcεRI receptors were designed based on this analysis. The amino acid residues exchanged between FcγRIIIB and FcεRI in the chimeras are boxed. Residues involved in ligand binding in FcγRIIA are boxed on that sequence.

Monoclonal antibodies to CD16 (3G8 (37), CLB-Fcgran1 (38), DJ130c, MEM-154, LNK16, and B88-9) were clustered and characterized in the Fifth International Workshop of Leukocyte Differentiation Antigens (22). W6/32 (39) reacts with a monomorphic determinant of human HLA-A, B, and was used as a positive control.

IgG Complexes, Dimers, and IgE—Human IgG1 protein was purified from the sera of a myeloma patient by (NH₄)₂SO₄ precipitation and *Staphylococcus aureus* protein A-Sepharose CL-4B (Pharmacia, Freiburg, Federal Republic of Germany) affinity column, prepared according to the manufacturer's instructions. IgG1 was aggregated by heating at 65 °C for 20 min at the concentration of 1 mg/ml resulting in about 50% of complexed protein. The complexes were purified from monomers by size exclusion high pressure liquid chromatography on a TSK-3000 SWXL column (Supelco, Bad Homburg, Germany). The fractions of separated IgG complexes were further analyzed by agarose-SDS-polyacrylamide gel electrophoresis (0.5% agarose, 1.5% polyacrylamide, 0.1% SDS) that revealed only high molecular mass (≥1000 kDa) complexes. Dimers and smaller polymers were not detectable by this analysis. hIgG1 dimers were prepared by chemical cross-linking with bis(sulfosuccinimidyl)-suberate (Pierce, Köln, Germany) according to manufacturer's instructions. Briefly, 10 mg of hIgG1 (10 mg/ml) in phosphate-buffered saline was incubated with 4 mg of bis(sulfosuccinimidyl)-suberate for 30 min at room temperature. The reaction was terminated by adding Tris buffer (pH 7.0) up to a final concentration of 50 mM. Excess of the reagents was removed by centrifugation with the Centricon 50 microconcentrator (Amicon, Witten, Germany). Cross-linked IgG1 dimers were purified from monomers and higher polymers by size exclusion chromatography on a Bio-Gel A-5m (BIO-RAD Laboratories, Munich, Germany) column (80 × 1.6 cm). Fractions containing monomers, dimers, and polymers, respectively, were collected and concentrated using Centrprep 30 (Amicon). Purity of isolated dimers was monitored by high pressure liquid chromatography analysis on the size exclusion column TSK-3000 SWXL. IgG molarities in the binding assays with dimers and the heat-aggregated complexes were calculated by assuming the molecular mass of hIgG1 monomers (150 kDa; Ref. 40), regardless of the degree of polymerization.

Human myeloma cell line SKO-007 (41) secreting IgE was a gift from Dr. R. Lamers (Max Planck Institute for Immunobiology, Freiburg, Germany). The cells were cultured in Iscove's modified Eagle's medium (Life Technologies, Inc., Eggenstein, Germany) supplemented with 1% fetal calf serum (PAA, Linz, Austria), 2 mM L-glutamine, 100 units/ml penicillin, 100 μg/ml streptomycin (Biochrom KG, Berlin, Germany). IgE was purified from culture supernatants on a NHS-activated HiTrap column (Pharmacia) coupled with polyclonal antibody to hIgE (The Binding Site, Heidelberg, Germany).

Construction of Chimeric FcγRIIIB/FcεRI and Mutant FcγRIIIB cDNAs—Chimeric (several amino acid residues) and mutant (single residues were replaced in FcγRIIIB with the equivalent ones in FcεRI sequence) cDNAs were created by oligonucleotide-directed mutagenesis as described in the M13 *in vitro* mutagenesis kit (Amersham, Braunschweig, Germany). The 568-bp *SphI-KpnI* fragment (nucleotides 53–620) coding for the extracellular part of FcγRIIIB was subcloned into M13 mp18. This clone was used as a single-stranded template for mutagenesis with specific oligonucleotides of 30–43 bp for chimeras and 18–20 bp for mutant receptors. "Silent" restriction sites were designed into the oligonucleotides to facilitate screening for the respective mutants. The presence of mutations was further confirmed by polymerase chain reaction sequencing with the fmol DNA sequencing kit (Promega). Mutated DNA fragments encoding for the extracellular part were excised from M13 with *SphI* and *KpnI* and cloned back into the pCDM8 expression vector containing the additional parts of the original FcγRIIIB cDNA.

Chimeric FcγRIIIB/B receptor was constructed by cloning the 536-bp *SphI-HincII* fragment coding for the extracellular part of the FcγRIIIB gene into the FcγRIIIB gene.

Cells and Transient Transfection—293 cells, an Adenovirus type 5-transformed primary human embryonic kidney cell line (42), were used for transient transfection with the Ca₃(PO₄)₂ method (43). Briefly, plasmid DNA was precipitated with 2 M CaCl₂ and HEPES-buffered saline (140 mM NaCl, 0.75 mM Na₂HPO₄, 50 mM HEPES, pH 7.14). Cells (30–50% confluent per 10-cm Petri dish) were incubated with the DNA (2 μg/ml) in Dulbecco's modified Eagle's medium NUT FIX-12 (Life Technologies, Inc.) supplemented with 10% fetal calf serum, 2 mM L-glutamine, 100 units/ml penicillin, 100 μg/ml streptomycin for 6 h. After removal of the transfection medium, the cells were treated with 15% glycerol in HEPES-buffered saline for 2 min at 37 °C, washed twice, and incubated in culture medium for 30–36 h before harvesting.

IgG Binding Assays and Flow Cytometry—Transfected cells were harvested with 1 mM EDTA in phosphate-buffered saline and washed with phosphate-buffered saline containing 0.2% bovine serum albumin (Serva, Heidelberg, Germany), and 1 × 10⁵ cells were assayed for binding with serial dilutions of hIgG1 complexes (6–300 nM) or dimers (0.06–1.2 μM) at 4 °C for 1 h. Incubations with CD16 mAbs and hIgE were performed under the same conditions. Immunoglobulin fractions bound were quantified with fluorescein isothiocyanate-labeled secondary antibodies to human or mouse IgG (Dianova, Hamburg, Germany) and human IgE (ICN Biochemicals, Meckenheim, Germany) using a FACScan equipped with a single argon-ion laser (Becton Dickinson, Mountain View, CA).

Molecular Modeling of FcγRIIIB—Sequence multialignment between FcγRIIIB and various immunoglobulin molecules revealed that the receptor adopts an Ig-fold. Using the alignment, we defined a secondary structure of the receptor and predicted general structural features. The three-dimensional molecular model of the two domains of FcγRIIIB was developed based on homology with the known structure of a human myeloma IgG molecule (44). The x-ray crystallographic structure of this antibody Fab fragment is available in the Brookhaven Protein Data Bank. Molecular modeling, minimization of energy, as well as other structural manipulations were carried out using the BIOSYM program.

RESULTS AND DISCUSSION

Mapping of the Regions Involved in IgG Binding on the Membrane-proximal Domain of FcγRIIIB—Mutational analysis of the FcγRIIIB was based on two hypotheses. First, β-turns of the Ig-like extracellular domains of the receptor could be the most probable sites for ligand binding; second, dissimilar amino acids in the extracellular parts of the highly homologous receptors, FcγRIIIB and FcεRIα, might perform the basis for different ligand binding properties. The membrane-distal domain of FcγRIIIB was shown not to be involved in ligand binding (35). Therefore, only the second, membrane-proximal domain of FcγRIIIB was subjected to the β-turn probability prediction using the Chou and Fasman algorithm (45) in the PC Gene program (Fig. 1). In the amino acid sequence comparison of FcγRIIIB and FcεRIα, the putative β-turns revealed a relatively high degree of dissimilarity, and these regions in FcγRIIIB were chosen for substitution with the equivalent residues of the FcεRIα sequence (Fig. 1). The amino acid exchanges in the chimeric receptors are indicated in Fig. 1 and Table I. The chimeras are designated according to the position of the residues substituted on the FcγRIIIB sequence.

The wild-type and chimeric receptors were transiently expressed in 293 cells, and the structural integrity of the receptors was assessed with a panel of six CD16 mAbs (3G8, DJ130c, Gran1, MEM-154, LNK16, and B88-9). No significant differ-

TABLE I
Reactivity of the chimeric and mutant receptors with CD16 mAbs and hIgG1

Amino acids exchanged in chimeric and mutant receptors are numbered according to their location in the FcγRIIIB sequence. Relative expression levels of the mutants were determined considering the reactivity with CD16 mAbs. Reactivity to mAbs was calculated as % of mean fluorescence intensity measured for the wt FcγRIIIB transfectants with the same mAb in the same experiment and shown as □ for 70–100%, ▣ for 40–70, and ■ for 0–40% of the reactivity with the wild-type receptor. The K_d values were calculated by non-linear regression analysis using Kaleidagraph 2.0.2 software. The receptor-ligand binding curve and K_d calculations were carried out, according to the formula $y = (B_{\max} \times (FL - FL_{\text{neg}})) / (K_d + (FL - FL_{\text{neg}}))$, where B_{\max} is the cell receptor number, FL is anti-IgG fluorescence of the given receptor at the provided ligand concentration, FL_{neg} is anti-IgG fluorescence in the absence of IgG, and K_d is the dissociation constant for receptor-IgG interaction. The values for B_{\max} are indicated as % of B_{\max} of wt receptor in each separate experiment. The values are presented as means of three separate experiments, and significantly lowered K_d values are shown in bold. ND, not detected; NT, not tested.

Receptor	Amino acids substituted	Level of expression wt ± S.D.	Reactivity with CD16 mAbs							Binding of hIgG1		
			3G8	DJ130c	Gran1	MEM-154	LNK16	B88-9		K_d ± S.D.		B_{\max} wt ± S.D.
										Complexes	Dimers	
		%								nM		%
wt FcγRIIIB		100	□	□	□	□	□	□	53.1 ± 6.8	460 ± 30	100	
Chimera												
FcγRIIIA/B		105 ± 10	□	□	□	□	□	□	50.7 ± 7.6	270 ± 70	98.3 ± 5.6	
97-99	PRW - SAE	120 ± 17	□	□	□	□	□	□	57.5 ± 11.7	NT	112.5 ± 11.5	
113-118	SWKNTA - GWRNWD	82 ± 7	▣	□	■	■	▣	■	ND	NT	ND	
125-127	LQN - YKD	125 ± 13	□	□	□	□	□	□	150.0 ± 44.2	5510 ± 480	77.3 ± 13.4	
129-131	KDR - EAL	118 ± 10	□	□	□	□	□	□	48.1 ± 1.5	380 ± 30	91.0 ± 5.9	
134-138	FHHNS - WYENH	93 ± 5	▣	□	▣	▣	■	▣	ND	NT	ND	
147-148	LK - VE	105 ± 11	□	□	□	□	□	□	61.5 ± 7.2	NT	94.3 ± 7.5	
152-158	SYFCRGL - TTYCTGK	92 ± 8	□	□	□	□	□	□	86.0 ± 19.8	2900 ± 730	74.5 ± 8.6	
160-163	GSKN - WQLD	76 ± 13	■	□	▣	▣	□	■	ND	ND	ND	
Mutant												
125	L - Y	94 ± 9	□	□	□	□	□	□	182.3 ± 50.9	1400 ± 260	77.8 ± 11.2	
126	Q - K	115 ± 11	□	□	□	□	□	□	116.6 ± 7.1	2570 ± 630	79.0 ± 4.4	
127	N - D	112 ± 18	□	□	□	□	□	□	50.1 ± 8.1	NT	94.9 ± 15.4	
154	F - Y	93 ± 7	□	□	□	□	□	□	71.1 ± 4.8	750 ± 30	93.6 ± 6.2	
156	R - T	127 ± 14	□	□	□	□	□	□	ND	ND	ND	
158	L - K	101 ± 9	□	□	□	□	□	□	50.0 ± 6.3	NT	105.1 ± 3.6	
161	S - Q	117 ± 12	□	□	□	□	□	□	65.2 ± 9.6	NT	121.6 ± 7.9	
162	K - L	110 ± 12	▣	□	□	□	□	▣	143.3 ± 34.2	1510 ± 270	81.6 ± 11.2	
163	N - D	103 ± 8	□	□	□	□	□	□	66.4 ± 10.4	200 ± 50	93.5 ± 7.1	
164	V - Y	118 ± 15	■	□	□	□	□	■	ND	ND	ND	
165	S - E	90 ± 7	□	□	□	□	□	□	69.5 ± 8.9	NT	94.6 ± 8.7	

ences between the interaction with wild-type FcγRIIIB and five of the eight chimeras were observed with the mAbs (Table I), indicating that the mutations had caused no major alterations in the structure of these chimeric receptors. In contrast, the chimera 160–163 was not recognized by the ligand-binding inhibitory mAb 3G8, and the binding with the mAbs Gran1, MEM-154, and B88–9 was affected (about 30–60% of wild-type receptor). mAb DJ130c reacted at the wild-type level with all the chimeras (Table I). Recognition of two chimeric receptors, 113–118 and 134–138, was significantly decreased by most of the CD16 mAbs (Table I). Thus, we assumed extensive structural alterations in the membrane-proximal domains of these receptors.

The epitopes for the mAbs used have not been extensively studied yet. DJ130c is considered to bind the membrane-distal domain of FcγRIII (46). This explains the reactivity of the antibody with all the chimeras. The other five mAbs used are directed against the membrane-proximal domain (46).² 3G8 is known to interfere with the ligand binding of the receptor (37, 46). Thus, the complete loss of binding with 3G8 indicates a major alteration within the IgG binding site on the chimera 160–163.

In binding assays of transfected 293 cells with hIgG1 com-

plexes, a K_d of 53.1 nM was calculated for the wild-type FcγRIIIB (Table I). The affinity of the receptor to covalently linked highly purified hIgG1 dimers was about 10 times lower ($K_d = 4.6 \times 10^{-7}$ M, Table I), presumably due to the lower valency of the dimeric ligand.

A FcγRIIIA/B chimera that maintained the extracellular domains of FcγRIIIA in the glycosylphosphatidylinositol-anchored molecule revealed similar to wild-type FcγRIIIB affinities to IgG1 complexes ($K_d = 50.7$ nM, Table I and Fig. 2) as well as to dimers ($K_d = 2.7 \times 10^{-7}$ M, Table I). Hence, we suppose that the minor differences in the amino acid sequences of the extracellular domains of these two isoforms do not account for the higher IgG binding capacity of FcγRIIIA (20).

293 cells bearing the chimeras 97–99, 129–131, and 147–148 showed binding affinities similar to wt FcγRIIIB (Fig. 2). In contrast, chimeras 125–127 and 152–158 bound hIgG1 complexes as well as dimers at significantly lower levels (K_d values for the chimeras are shown in Table I). Chimera 160–163 had almost completely lost the capacity to bind IgG (Fig. 2). Since this chimera was still recognized by most of the CD16 mAbs except 3G8, we speculate that we have rather replaced residues functional in ligand and 3G8 binding than destroyed the overall structure of the second domain.

Binding affinities of the receptors to chemically cross-linked IgG dimers were lower than to heat-aggregated complexes

² A. Tamm and R. E. Schmidt, manuscript in preparation.

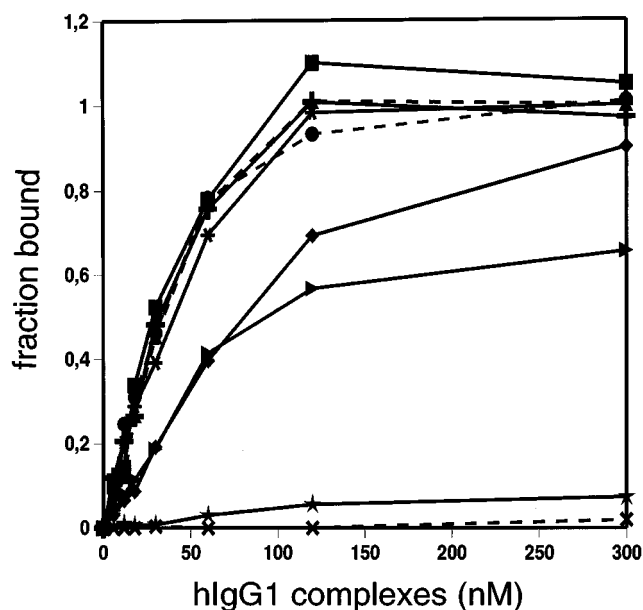


FIG. 2. Binding of the chimeric receptors to hIgG1 complexes. Binding of serial dilutions of heat-aggregated hIgG1 to 293 cells transfected with cDNAs of wt FcγRIIIB (●, dashed line), chimeras FcγRIIIA/B (▲, dashed line), 97–99 (■), 125–127 (◆), 129–131 (✦), 147–148 (*), 152–158 (▶), 160–163 (★), and of mock cells (✕, dashed line). The panel represents results of a typical experiment. Fraction of bound IgG1 was calculated according to the formula $f = \frac{FL - FL_{neg}}{FL_{wt(max)} - FL_{wt(neg)}}$, where FL = anti-IgG fluorescence of the given receptor at the provided concentration of IgG complexes, FL_{neg} = anti-IgG fluorescence in the absence of IgG, and $FL_{wt(max)}$ = anti-IgG fluorescence of the wt FcγRIIIB at saturation. Binding assays were performed in triplicates.

(Table I). However, the chimeric receptors reacted with hIgG1 dimers and large complexes in the same manner, *i.e.* the chimeras 127–127, 152–158, and 160–163 revealed decreased binding capacities to both the ligands, whereas the other three chimeras (97–99, 129–131, and 147–148) showed binding affinities comparable to the wild-type FcγRIIIB.

Chimeras 113–118 and 134–138 did not bind IgG as well as most of the CD16 mAbs mapped to react with the membrane-proximal domain. As discussed below, the loss of IgG binding was considered to result from the destroyed structure of the domain, and these chimeras were excluded from further mutational analysis.

None of the transfectants expressing chimeric receptors were able to interact with hIgE (data not shown). Evidently, the FcεRI-derived amino acid residues in the chimeras are not directly involved in IgE binding or are not sufficient for the binding detectable in our assays.

Localization of the Putative IgG Binding Regions on the Molecular Model of the Membrane-proximal Domain of FcγRIIIB—Since there has been no solution to the three-dimensional structure of FcγRIII yet, the FcγRIIIB NA2 allele was computer-modeled in this study. The model demonstrates the membrane-proximal domain of the receptor as a typical Ig-like molecule with seven antiparallel β-sheets that are arranged in ABE and GFC surfaces (Fig. 3). The C' β-sheet between the C and E sheets may be important for connecting both the surfaces. According to the model, amino acids that were shown to be crucial for ligand binding by chimeric receptors are located on the CC' loop (125–127) and on the FG loop (160–163, Fig. 3). Residues replaced in the chimera 152–158 (Ser¹⁵², Phe¹⁵⁴, Arg¹⁵⁶, and Leu¹⁵⁸) were found to be located on the F β-sheet and conformationally placed between the two loops involved (Fig. 3). The model is in concordance with the

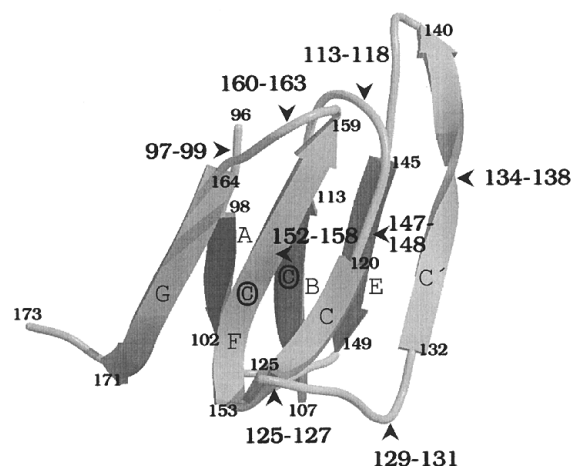


FIG. 3. Molecular model of the membrane-proximal domain of FcγRIIIB. Ribbon diagram presentation of a "MOLSCRIPT" (58) and "RASTER three-dimensional" (59) drawing showing the predicted β-strands G, F, C in the front (light) and A, B, E in the back (dark). The regions that were replaced with the equivalent ones from the FcεRIα in the chimeric receptors are indicated. The cysteines that form the disulfide bond are shown on F and B β-sheets.

data of our mutation analysis, demonstrating that these three regions may constitute one conformational binding site for IgG, located on the GFC β-sheet surface.

Amino acids substituted in the chimeras that did not have any effect on ligand binding (97–99, 129–131, and 147–148) are positioned apart from the binding surface on this model. Residues 97–99 stretch between the two extracellular domains, and 147–148 are located on the E β-sheet. Both the regions are located on the ABE surface of the membrane-proximal domain, thus on the opposite side of the potential binding area (Fig. 3). Residues 129–131 are placed on the CC' loop, opposite to the 125–127 region. Replacement of these amino acids seems not to affect the function of the neighboring putative binding residues 125–127, since the substitution did not influence the interaction with IgG (Table I, Fig. 2).

The overall structure of two of the chimeric receptors (113–118 and 134–138) was considered to be disrupted according to the monoclonal antibody data. Location of the amino acids 134–138 on the C' β-sheet that is presumably stabilizing the two β-sheet surfaces would explain the disruption of the structure of the domain when these residues were substituted. According to the model, the region 113–118 within the BC loop is also connecting the two β-sheet surfaces and, therefore, likely to be stabilizing the conformation of the domain. In addition, this region can be involved in generating the binding site due to the close proximity to the FG loop, the potential binding structure for IgG.

The GFCC' surface of the membrane-proximal domain of hFcγRII has been reported to be crucial for IgG binding (1). The key residues on hFcγRIIA (Fig. 1) are shown to locate on the FG loop of the domain on a molecular model of this receptor (1). The FG loop is also involved in ligand binding in mouse FcγRII (32, 33). These data support our hypothesis that the FG loop of the membrane-proximal domain is the main binding determinant in FcγRIII, as was demonstrated by the loss of IgG binding capacity after substituting the residues 160–163 on the putative FG loop.

Arg/His¹³¹ influences the interaction of hFcγRIIA with hIgG2 (47, 48). The low responsive FcγRIIA isoform harbors histidine in this position and interacts with human IgG2 but not with mouse IgG1, whereas arginine in the position 131 in FcγRIIA abolishes the binding to hIgG2. Arg/His¹³¹ is located on the C'E loop on the FcγRIIA model (1). In hFcγRIII, His¹³⁵

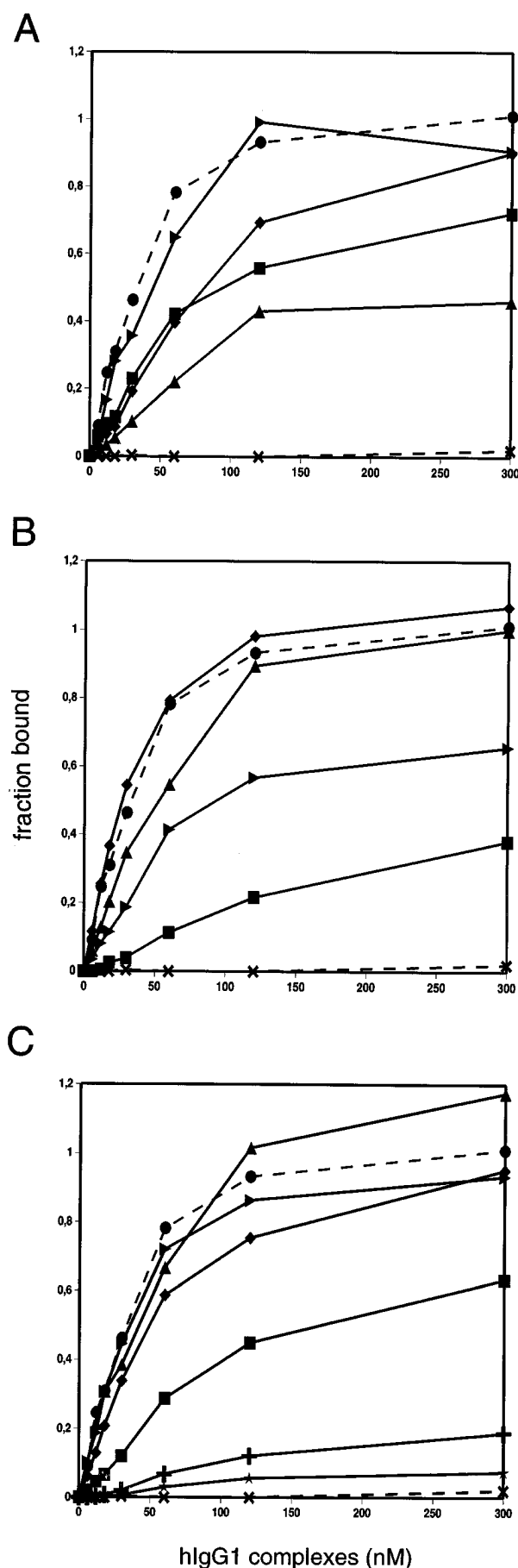


FIG. 4. Binding of the single residue mutant receptors to hIgG1 complexes. Representative IgG1 binding experiments of the

is corresponding to the His/Arg¹³¹ in hFcγRIIA (Fig. 1) and is putatively positioned on the C' β-sheet. Since hFcγRIII does not bind IgG2 and, according to our model, the C' β-sheet remains conformationally distant from the GFC surface, we suggest the residues on this β-sheet are not directly involved in hIgG1 binding.

Detailed Structure Analysis of the Potential Binding Site—The three amino acid regions (125–127, 152–158, and 160–163) demonstrated to be involved in IgG binding by chimeric receptors and the molecular model were subjected to further mutational analysis. Site-directed mutagenesis of 11 single residues was carried out (Table I). Similarly to the chimeras, each residue was substituted with the equivalent one of the FcεRI sequence.

Within the region 125–127 (LQN–YKD), replacement of Leu¹²⁵ with Tyr and of Gln¹²⁶ with Lys resulted in lower IgG binding capacities ($K_d = 182$ and 116 nM for IgG complexes, respectively, Table I, Fig. 4A), comparable to that of the responsive chimera ($K_d = 150$ nM). In contrast, changing Asn¹²⁷ to Asp did not alter the binding affinity of the mutant receptor (Fig. 4A, Table I). Interaction with IgG1 dimers followed the same pattern, *i.e.* mutants Leu¹²⁵ and Gln¹²⁶ harbored decreased ligand binding capacities as compared to the wild-type receptor. Analyzing the receptor model, we supposed that only Glu¹²⁶ and not Leu¹²⁵ is directly involved in binding. We assume that replacing the small polar side chain of leucine with that of aromatic tyrosine in the mutant Leu¹²⁵ has led to immense structural changes in the CC' loop and, thus, to interrupted ligand binding.

An IgG binding site of FcγRIIIB has been described by Hibbs *et al.* (35) who identified a continuous binding region on the CC' loop of the second domain, Gln¹²⁶–Tyr¹³³, by alanine-scanning mutagenesis. In contrast to these data, our mutational analysis revealed no linearly continuous binding sites. In our experiments, replacement of the sequence Lys¹²⁹–Asp–Arg¹³¹ with Glu–Ala–Leu from FcεRI did not influence IgG binding. Only conversions of the polar Leu¹²⁵ and Gln¹²⁶ (Fig. 6) to aromatic Tyr or positively charged Lys, respectively, disrupted ligand-receptor interaction, whereas changing the charge of the adjacent side chain (NH₂ group of Asn¹²⁷ to negatively charged O[−] of Asp) did not affect the interaction at all. We suppose that substitution of every amino acid to alanine by Hibbs *et al.* (35) affected the structure of the CC' loop and, hence, the binding capacity, even when the residues neighboring to functional ones were changed. Gly¹²⁸ was also recognized to be involved in IgG binding in that study. Glycine with only one hydrogen atom as the side chain can adopt a wider range of main chain conformations than other residues (28) and should play an important role in maintaining the structure of the CC' loop. This might as well explain the absence of ligand binding by mutated Gly¹⁵¹, also demonstrated in that study (35).

We constructed three mutants (Phe¹⁵⁴, Arg¹⁵⁶, and Leu¹⁵⁸) in the second region, 152–158. Analyzing the molecular model, Ser¹⁵² was found to be placed apart from the other residues and excluded from further studies. Replacement of the positively charged Arg¹⁵⁶ (Fig. 4B, Table I) with polar Thr resulted in the decrease of receptor function, while exchanging the neighboring residues Phe¹⁵⁴ with Tyr and Leu¹⁵⁸ with Lys did not have

mutant receptors are grouped according to the chimeras they originate from. Panel A, 293 cells were transfected with cDNAs of wt FcγRIIIB (●, dashed line), chimera 125–127 (◆), mutant receptors Leu¹²⁵ (▲), Gln¹²⁶ (■), Asn¹²⁷ (▶), and vector DNA (×, dashed line). Panel B, transfectants of wt FcγRIIIB (●), chimera 152–158 (★), Phe¹⁵⁴ (▲), Arg¹⁵⁶ (■), and Leu¹⁵⁸ (◆). Panel C, transfectants of wt FcγRIIIB (●), chimera 160–163 (▶), Ser¹⁶¹ (▲), Lys¹⁶² (■), Asn¹⁶³ (◆), Val¹⁶⁴ (✦), and Ser¹⁶⁵ (★). Experiments were performed in triplicates, and fractions bound were calculated as described in Fig. 2.

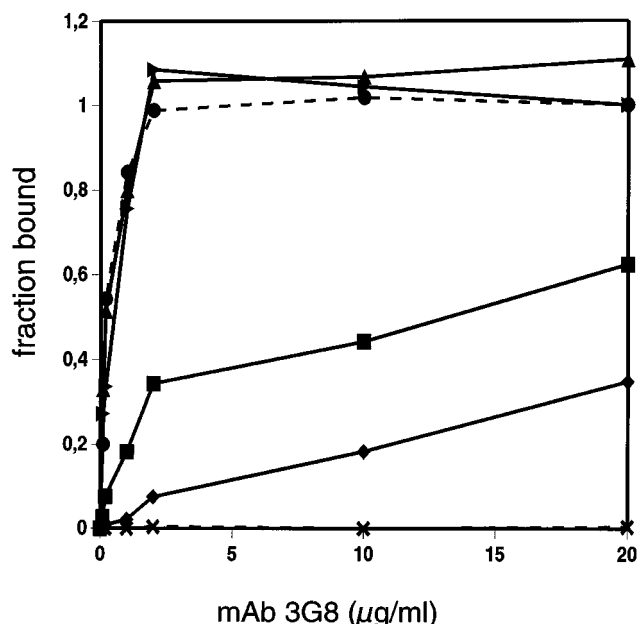


FIG. 5. **Binding of transfectants with mAb 3G8.** 293 cells transfected with the cDNAs of wt FcγRIIIB (●, dashed line), mutant receptors Lys¹⁶² (■), Val¹⁶⁴ (◆), Gln¹²⁶ (▲), Arg¹⁵⁶ (▴), and vector DNA (×, dashed line) were incubated with serial dilutions of 3G8 (0.1–20 µg/ml). Bound mAb was detected with fluorescein isothiocyanate-labeled anti-mouse antibody by fluorescence-activated cell sorter analysis. Fractions of 3G8 bound were calculated as described in the legend for Fig. 2.

significant effects on IgG binding. Substitution of only the Arg¹⁵⁶ with Thr disrupted receptor-ligand interaction to a considerably higher extent than did the replacement of the longer region, 152–158 (Table I, Fig. 4B). We assume that the single residue replacement destroyed also the possible β -sheet structure and ablated IgG binding capacity of the receptor. In contrast, when the whole F β -sheet was exchanged in the chimera 152–158, IgG binding was decreased, apparently, due to the missing of the residue of direct interaction with the ligand.

Based on the chimera 160–163, the amino acid Ser¹⁶¹ was converted to Gln, Lys¹⁶² to Leu, Asn¹⁶³ to Asp, Val¹⁶⁴ to Tyr, and Ser¹⁶⁵ to Glu. Two of the substitutions, Lys¹⁶² to Leu and Val¹⁶⁴ to Tyr, resulted in decreased ligand binding capacities of the respective receptors. The mutation of Val¹⁶⁴ almost abolished the ability to bind IgG (Fig. 4C, Table I). Both the mutants reacted weakly with the mAbs 3G8 and B88–9, indicating that Lys¹⁶² and Val¹⁶⁴ are located also within the epitopes for these antibodies. The three other mutant receptors, Ser¹⁶¹, Asn¹⁶³, and Ser¹⁶⁵, resembled the wild-type receptor (Fig. 4C, Table I), although in every instance a substantial change in charge and/or configuration of the side chain was generated. We conclude that Lys¹⁶² and Val¹⁶⁴, which are located according to the molecular model on the FG loop, are crucial for IgG binding, either being involved in direct interactions with the ligand or determining the conformation of the FG loop.

Binding Epitope of the mAb 3G8—The chimera 160–163 was not recognized by mAb 3G8, the mostly used ligand-binding inhibitory antibody to CD16 (Table I). Hence, these residues within the FG loop of the second domain are likely to constitute the binding epitope for the antibody. Among the single residue mutants, 3G8 reacted poorly with Lys¹⁶² and Val¹⁶⁴ (Table I, Fig. 5). Other mutants of this region Ser¹⁶¹, Asn¹⁶³, Ser¹⁶⁵, as well as Gln¹²⁶ and Arg¹⁵⁶, which presented disrupted IgG binding capacities, reacted at a level comparable to that of the wild-type receptor (Table I, Fig. 5). 3G8 binding studies, performed with serial dilutions of the antibody, demonstrated that the interaction was more profoundly interrupted with the mu-

tant Val¹⁶⁴ (Fig. 5). The same was observed for the binding of IgG1 (Figs. 5 and 4C, respectively) and for another mAb, B88–9. B88–9 is known to interfere with 3G8-FcγRIII binding (46), sharing apparently an overlapping epitope with 3G8. It is likely that the residues Lys¹⁶² and Val¹⁶⁴ belong to a non-linear binding epitope for the inhibitory antibody as well as for IgG. On the other hand, the FG loop may compose a conformational binding site for the ligand as well as for the monoclonal antibodies 3G8 and B88–9, and thus, alteration of the structure of the loop could influence the binding capacity of the receptor.

hFcγRIII-IgG Interaction—In this study, the key residues for ligand binding of the FcγRIIIB are assumed to be located on the GFC face of the membrane-proximal domain (Figs. 3 and 6). The GFC surface remains distant from the first, membrane-distal domain on our molecular model of FcγRIIIB. Using the space-filling presentation of the membrane-proximal domain, the side chains of the four residues implicated (Gln¹²⁶, Arg¹⁵⁶, Lys¹⁶², and Val¹⁶⁴) are exposed extending to the surface of the molecule (Fig. 6). According to the model, they could belong to one discontinuous binding site for IgG. Replacement of the amino acids Lys¹⁶² and Val¹⁶⁴ on the FG loop demonstrated the most profound effect on ligand binding (Table I), indicating that the FG loop is the main binding determinant on FcγRIII. The same GFCC" surface and essentially FG loop were also shown to be critical for binding on the hFcγRII receptors (1, 5), providing an additional support to our data.

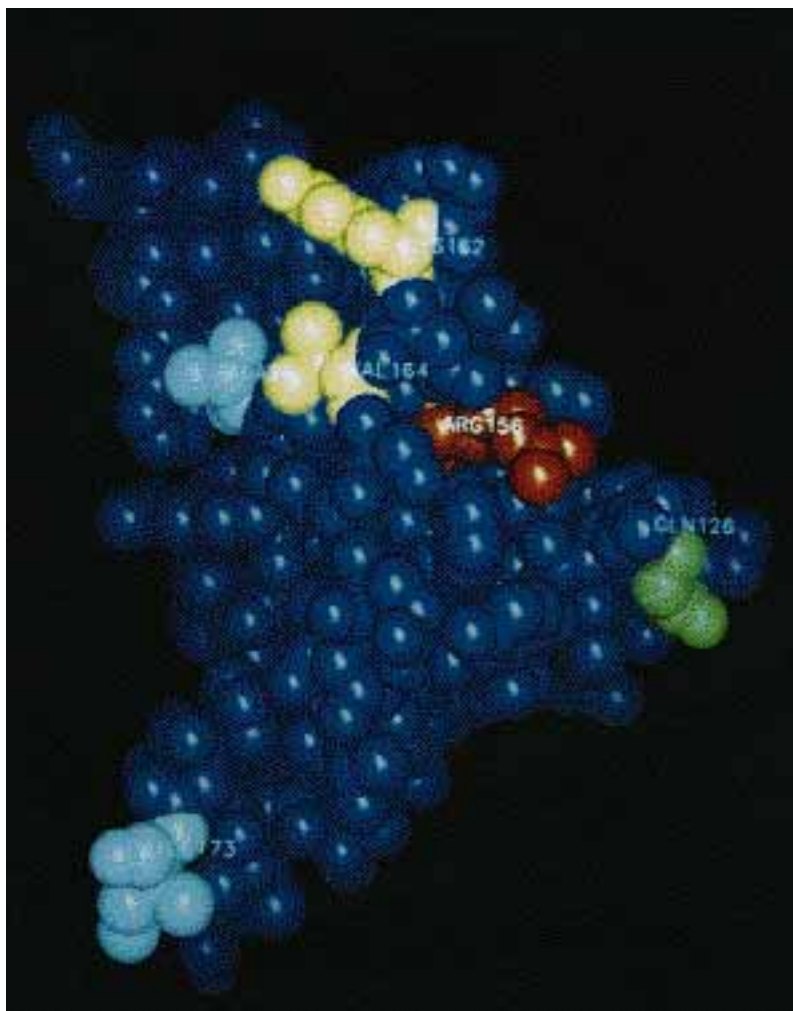
On IgG1 and IgG3, the natural ligands for these receptors, the lower hinge region (amino acids 233–237) has been identified to constitute a binding pocket for all Fcγ receptors (49–52). The lower hinge regions are different in IgG2 and IgG4, which explains also the failure of these subclasses to interact with Fcγ receptors. Based on these data, we suppose that the same structural elements on the low affinity Fcγ receptors, *e.g.* FG loops, are interacting with the same binding site, the lower hinge region on the IgG molecules. Although the amino acid residues found to be involved in ligand binding in FcγRIIIB are not conserved among Fc receptors (Fig. 1), we think that the FG loops of the membrane-proximal domains of different Fcγ receptors constitute similar binding structures for IgG, whereas different single residues are involved in direct interactions.

The extensive amino acid sequence homology between FcεRI and Fcγ receptors suggests that a similar folding pattern might be adopted by these receptors, and the FG loops could be even more widely used as an interaction site with immunoglobulins.

A relatively higher affinity to IgG has been reported for the FcγRIIIA receptor (19, 20). The minor differences in the extracellular polypeptide sequences of the FcγRIII A and B were shown not to be responsible for the improved binding capacity of the A isoform, since the chimera FcγRIIIA/B harboring the extracellular part of the A isoform in the B gene bound hIgG1 complexes and dimers similarly to the FcγRIIIB. An additional binding site for FcγRIIIA has been proposed in the CH3 domain of IgG (53–55). Binding curves obtained in our experiments do not refer to the existence of a second binding site on FcγRIIIB. However, the possibility remains to be studied that on NK cells, which express FcγRIIIA in association with the γ -chain of the FcεRI, the receptor exposes different interaction characteristics with IgG and thus endures higher affinity to the ligand.

Understanding the molecular basis of the interactions between Fcγ receptors and immunoglobulins is of great importance, since the use of antibodies as therapeutic agents is increasing. The low affinity Fcγ receptors are also believed to play an important role in inducing antibody-mediated inflammation (56, 57). Several chronic inflammatory diseases like rheumatoid arthritis and leukocytoclastic vasculitis are linked to constant presence of antigen-antibody complexes and con-

FIG. 6. Space-filling presentation of the ligand binding domain of Fc γ RIIIB. Amino acid residues putatively involved in IgG binding are colored. The N (Leu⁹³) and C termini (Ile¹⁷²) of the domain are indicated by cyan. The computer model was generated based on the previously described structure of a IgG Fab fragment (44).



tinuous activation of effector cells expressing Fc γ receptors. Identification of the binding sites on the receptors may provide new possibilities for treatment of these diseases by blocking Fc γ receptor-IgG interaction.

Acknowledgments—We thank Dr. B. Seed for the Fc γ RIIIB cDNA, Dr. W. Bautsch, Dr. R. Sillard, and Dr. B. Hipskind for stimulating discussions and critical reading of the manuscript, Dr. J. Alves for the help in visualizing the receptor model, and C. Schiller and G. Bassman for assistance in IgG binding assays.

REFERENCES

- Hulett, M. D., Witort, E., Brinkworth, R. I., McKenzie, I. F. C., and Hogarth, P. M. (1994) *J. Biol. Chem.* **269**, 15287–15293
- Unkeless, J. C., Scigliano, E., and Freedman, V. H. (1988) *Annu. Rev. Immunol.* **6**, 251–281
- Ravetch, J. V., and Kinet, J.-P. (1991) *Annu. Rev. Immunol.* **9**, 457–492
- Van de Winkel, J. G. J., and Capel, P. J. A. (1993) *Immunol. Today* **14**, 215–221
- Hulett, M. D., and Hogarth, P. M. (1994) *Adv. Immunol.* **57**, 1–127
- Huizinga, T. W., Kerst, M., Nuyens, J. H., Vlug, A., von dem Borne, A. E. G. Kr., Roos, D., and Tetteroo, P. A. (1989) *J. Immunol.* **142**, 2359–2364
- Van de Winkel, J. G. J., and Anderson, C. L. (1991) *J. Leukocyte Biol.* **49**, 511–524
- Ravetch, J. V., and Perussia, B. (1989) *J. Exp. Med.* **170**, 481–497
- Peltz, G. A., Grundy, H. O., Lebo, R. V., Yssel, H., Barsh, G. S., and Moore, K. W. (1989) *Proc. Natl. Acad. Sci. U. S. A.* **86**, 1013–1017
- Kurosaki, T., and Ravetch, J. V. (1989) *Nature* **342**, 805–807
- Lanier, L. L., Cwirla, S., Yu, G., Testi, R., and Phillips, J. H. (1989) *Science* **246**, 1611–1613
- Uciechowski, P., Gessner, J. E., Schindler, R., and Schmidt, R. E. (1992) *Eur. J. Immunol.* **22**, 1635–1638
- Lanier, L. L., Yu, G., and Phillips, J. H. (1989) *Nature* **342**, 803–805
- Simmons, D., and Seed, B. (1988) *Nature* **333**, 568–570
- Werfel, T., Uciechowski, P., Tetteroo, P. A. T., Kurrle, R., Deicher, H., and Schmidt, R. E. (1989) *J. Immunol.* **142**, 1102–1106
- Hundt, M., and Schmidt, R. E. (1992) *Eur. J. Immunol.* **22**, 811–815
- Gessner, J. E., Grussenmeyer, T., Kolanus, W., and Schmidt, R. E. (1995) *J. Biol. Chem.* **270**, 1350–1361
- Gessner, J. E., Grussenmeyer, T., and Schmidt, R. E. (1995) *Immunobiol.* **193**, 341–355
- Anderson, C. L., Looney, R. J., Culp, D. J., Ryan, D. H., Fleit, H. B., Utell, M. J., Frampton, M. W., Manganiello, P., and Guyre, P. M. (1990) *J. Immunol.* **145**, 196–201
- Vance, B. A., Huizinga, T. W. J., and Guyre, P. M. (1992) *FASEB J.* **6**, 1620
- Vance, B. A., Huizinga, T. W. J., Wardwell, K., and Guyre, P. M. (1993) *J. Immunol.* **151**, 6429–6439
- Huizinga, T. W. J., Kleijer, M., Roos, D., and van dem Borne, A. E. G. Kr. (1988) *Leukocyte Typing IV*, pp. 582–585, Oxford University Press, Oxford
- Schmidt, R. E. (1995) in *Leukocyte Typing V* (Schlossman, J., ed) Vol. 1, pp. 805–806, Oxford University Press, Oxford
- Ory, P. A., Goldstein, I. M., Kwok, E. E., and Clarkson, S. B. (1989) *J. Clin. Invest.* **83**, 1676–1681
- Huizinga, T. W. J., Kleijer, M., Tetteroo, P. A. T., Roos, D., and van dem Borne, A. E. G. Kr. (1990) *Blood* **75**, 1211–1214
- Salmon, J. E., Edberg, J. C., and Kimberly, R. P. (1990) *J. Clin. Invest.* **85**, 1287–1295
- Bredius, R. G. M., Fijen, C. A. P., de Haas, M., Kuijper, E. J., Weening, R. S., van de Winkel, J. G. J., and Out, T. A. (1994) *Immunology* **83**, 624–630
- Branden, C., and Tooze, J. (1991) *Introduction to Protein Structure*, Garland Publishing, Inc., New York
- Ierino, F. L., Hulett, M. D., McKenzie, I. F. C., and Hogarth, P. M. (1993) *J. Immunol.* **150**, 1794–1799
- Hulett, M. D., McKenzie, I. F. C., and Hogarth, P. M. (1993) *Eur. J. Immunol.* **23**, 640–645
- Mallamaci, M. A., Chizzonite, R., Griffin, M., Nettleton, M., Hakimi, J., Tsien, W.-H., and Kochan, J. P. (1993) *J. Biol. Chem.* **268**, 22076–22083
- Robertson, M. W. (1993) *J. Biol. Chem.* **268**, 12736–12743
- Hibbs, M. L., Hogarth, P. M., and McKenzie, I. F. C. (1985) *Immunogenetics* **22**, 335–348
- Lah, M., Quelch, K., Deacon, N. J., McKenzie, I. F. C., and Hogarth, P. M. (1990) *Immunogenetics* **31**, 202–206
- Hibbs, M. L., Tolvanen, M., and Carpen, O. (1994) *J. Immunol.* **152**, 4466–4474
- Kinet, J.-P., Metzger, H., Hakimi, J., and Kochan, J. (1987) *Biochemistry* **26**, 4605–4610
- Fleit, H. B., Wright, S. D., and Unkeless, J. C. (1982) *Proc. Natl. Acad. Sci. U. S. A.* **79**, 3275–3279
- Werner, G., von dem Borne, A. E. G. Kr., Bos, M. J. E., Tromp, J. F., van der

- Plas-van Dalen, C. M., Visser, F. J., Engelfriet, C. P., and Tetteroo, P. A. T. (1986) in *Leukocyte Typing II* (Reinherz, E. L., ed) p. 109, Springer-Verlag, New York
39. Barnstable, C. J., Bodmer, W. F., Brown, G., Galfre, G., Milstein, C., Williams, A. F., and Ziegler, A. (1978) *Cell* **14**, 9–12
 40. Carayannopolis, L., and Capra, D. J. (1993) in *Fundamental Immunology* (Paul, W. E., ed) pp. 283–314, Raven Press, New York
 41. Olsson, L., and Kaplan, H. S. (1980) *Proc. Natl. Acad. Sci. U.S.A.* **77**, 5429–5431
 42. Graham, F. L. (1977) *J. Gen. Virol.* **36**, 59–72
 43. Wigler, M., Silverstein, S., Lee, L.-S., Pellicer, A., Cheng, Y.-C., and Axel, R. (1977) *Cell* **11**, 223–232
 44. Saul, F. A., Amzel, L. M., and Poljak, R. J. (1978) *J. Biol. Chem.* **253**, 585–593
 45. Chou, P. Y., and Fasman, G. D. (1976) *Adv. Enzymol. Relat. Areas Mol. Biol.* **47**, 145–148
 46. de Haas, M., Kleijer, M., Roos, D., and Borne, A. E. G. Kr. (1995) in *Leukocyte Typing V* (Schlossman, J., ed) Vol. 1, pp. 811–814, Oxford University Press, Oxford
 47. Warmerdam, P. A., van de Winkel, J. G. J., Gosselin, E. J., and Capel, P. J. A. (1990) *J. Exp. Med.* **172**, 19–25
 48. Clark, M. R., Stuart, S. G., Kimberly, R. B., Ory, P. A., and Goldstein, I. M. (1991) *Eur. J. Immunol.* **21**, 1911–1916
 49. Duncan, A. R., Woof, J. M., Partridge, L. J., Burton, D. R., and Winter, G. (1988) *Nature* **332**, 563–564
 50. Lund, J., Winter, G., Jones, P. T., Pound, J. D., Tanaka, T., Walker, M. R., Artymuik, P. J., Arata, Y., Burton, D. R., Jefferis, R., and Roof, J. M. (1991) *J. Immunol.* **147**, 2657–2662
 51. Sarmay, G., Lund, J., Rozsnyay, Z., Gergely, J., and Jefferis, R. (1992) *Mol. Immunol.* **29**, 633–639
 52. Hindley, S. A., Gao, Y., Nash, P. H., Sautes, C., Lund, J., Goodall, M., and Jefferis, R. (1993) *Biochem. Soc. Trans.* **21**, 337S
 53. Sarmay, G., Jefferis, R., Klein, E., Benczur, M., and Gergely, J. (1985) *Eur. J. Immunol.* **15**, 1037–1042
 54. Lund, J., Tanaka, T., Takahashi, N., Sarmay, G., Arata, Y., and Jefferis, R. (1990) *Mol. Immunol.* **27**, 1145–1153
 55. Gergely, J., and Sarmay, G. (1990) *FASEB J.* **4**, 3275–3283
 56. Ravetch, J. R. (1994) *Cell* **78**, 553–560
 57. Kimberly, R. P., Salmon, J. E., and Edberg, J. C. (1995) *Arthritis Rheum.* **38**, 306–314
 58. Kraulis, P. J. (1991) *J. Appl. Crystallogr.* **24**, 946–951
 59. Bacon, D. J., and Anderson, W. F. (1988) *J. Mol. Graphics* **6**, 261–270